Conductance fluctuations in quantum wires

H. Tamura and T. Ando
Institute for Solid State Physics, University of Tokyo, 7-22-1 Roppongi, Minato-ku, Tokyo 106, Japan
(Received 11 December 1990; revised manuscript received 28 February 1991)

Conductance fluctuations in quantum wires are calculated numerically by a scattering-matrix formalism with Landauer's conductance formula. The fluctuations are not universal because they are strongly dependent on the system length. When many subbands are occupied, there appears the length region (called the universal region) longer than the mean free path and shorter than the localization length where the fluctuations are almost independent of the length. A crossover from one to two dimensions occurs when the broadening of one-dimensional subbands exceeds their separations. In the presence of a weak magnetic field, the universal region becomes wider and the fluctuations are reduced. In strong magnetic fields, the conductance becomes nearly quantized and the fluctuations become negligibly small due to the formation of edge states with an extremely long mean free path.

I. INTRODUCTION

Quantum transport phenomena have attracted much attention for years. In particular recent developments in experiments in mesoscopic submicrometer structures have revealed a quantum-mechanical nature of transport at low temperatures such as conductance fluctuations.[1] Conductance fluctuations were unexpectedly observed in the magnetoresistance of a small normal-metal ring,[2] instead of the Aharanov-Bohm oscillations predicted theoretically[3–5] and observed later.[6] These are the direct manifestation of quantum interference effects in systems with a size smaller than the phase-coherence length. More recently, various phenomena have been observed such as anomalies in the weak-field Hall effect[7–9] and the quantized conductance[10,11] also in quantum wires made at GaAs/$Al_xGa_{1-x}As$ heterostructures. In this paper we study numerically conductance fluctuations in quantum wires.

A special feature of conductance fluctuations is that although the fluctuating patterns are random as a function of the magnetic field B or the Fermi energy E_F, they are time independent, reproducible, and specific to each sample. Diagrammatic perturbation calculations[12–16] have shown that the amplitude of the fluctuations takes a universal value of order e^2/h, independent of sample size and degree of disorder at zero temperature, when the sample dimensions are always much larger than the mean free path l as well as the Fermi wavelength λ_F but are much smaller than the localization length ξ ("metallic system"). The universality has been shown by various other methods both analytically[17] and numerically.[18–27]

Different behaviors are expected in conductance fluctuations in quantum wires. In the quantum wires the width W is smaller than l and comparable to λ_F although the length is usually much larger than l. Therefore, the one-dimensional (1D) subbands are well defined and resolved because their level broadening is much smaller than their energy separation. Consequently, there is no definite transversal electron motion and we can no longer use the idea based on semiclassical Feynman paths valid in metallic wires. Moreover, the localization effect can be essential. As a matter of fact, in a strict 1D system the localization length ξ is comparable to the mean free path and therefore there is no diffusive regime where the conventional perturbation treatment is valid.[28–30] In wires with many conducting channels, the localization length becomes larger than the mean free path.

In this paper we study the behavior of conductance fluctuations in quantum wires by calculating the scattering matrix of the system containing impurities of δ-functional type in the presence of a magnetic field. We shall describe the theoretical formulation in Sec. II, present numerical results in Sec. III, and give a short summary in Sec. IV.

II. THEORETICAL MODEL

We consider a two-dimensional system of noninteracting electrons confined within the width W in the lateral (y) direction in the presence of a perpendicular magnetic field $\mathbf{B}$. The Hamiltonian is written as

$$H=\frac{1}{2m}(\mathbf{p}+e\,\mathbf{A})^2+U(y)+V(\mathbf{r})\ ,$$
$$U(y)=\begin{cases}0, & y<|W/2|\\ \infty, & y\geq|W/2|\end{cases}, \tag{2.1}$$

where $\mathbf{r}=(x,y)$, $\mathbf{A}=(-By,0)$, m is the effective mass, and $V(\mathbf{r})$ is the potential of impurities distributed randomly. The system has length L in the x direction and is connected on both ends to long perfect leads which themselves are connected to reservoirs. We assume the scattering potential from a single impurity as the δ function with the same strength $|\gamma|$, and do not take into account other scattering mechanisms, such as the long-range Coulomb scattering from an ionized impurity.[31]

In the absence of impurities the wave function is written as

$$\xi(\mathbf{r})\propto e^{ikx}\phi(y)\ , \tag{2.2}$$

where $\phi(y)$ satisfies the reduced equation

$$\left[-\frac{\hbar^2}{2m}\frac{d^2}{dy^2}+\frac{m}{2}\omega_c^2(y-l_B^2k)^2+U(y)\right]\phi(y)=E\phi(y)\ , \tag{2.3}$$

with $\omega_c=eB/m$ and $l_B^2=\hbar/eB$. For a given energy ($E=E_F$) we obtain the two kinds of mode, the "conducting mode" whose wave number is real, $\pm k_n$ ($n=1,2,\ldots,N_c;k_n>0$), and the "evanescent mode" whose wave number is imaginary, $\pm i\kappa_n$ ($n=N_c+1,N_c+2,\ldots,\infty;\kappa_n>0$). We denote the right-going waves consisting of the conducting modes with $+k_n$ or the evanescent modes with $i\kappa_n$ as ξ_{n+} and the left-going waves with $-k_n$ or $-i\kappa_n$ as ξ_{n-}.

The normalization of the conducting solution $\xi_{n\pm}$ is chosen as

$$\xi_{n\pm}(\mathbf{r})=\frac{1}{\sqrt{v_n}}e^{\pm ik_nx}\phi_{n\pm}(y)\ , \tag{2.4}$$

with the velocity in the x direction of the nth state given by

$$v_n=\frac{\hbar}{m}\int dy\,\phi_{n+}^*(y)\left[k_n-\frac{y}{l_B^2}\right]\phi_{n+}(y)\ , \tag{2.5}$$

so that each channel carries a unit flux. The normalization of the wave function of the evanescent channel is arbitrary and the conductance is independent of their choices.

The wave function can be written for the incoming wave from the left side of the scattering region $[0,L]$ as

$$\Phi_n^+(x,y)=\begin{cases}\xi_{n+}+\sum_{n'=1}^{N}\xi_{n'-}r_{n'n}, & x<0\\ \sum_{n'=1}^{N}\xi_{n'+}t_{n'n}, & x>L,\end{cases} \tag{2.6}$$

where t_{mn} and r_{mn} are the transmission and reflection amplitudes, respectively, and for the incoming wave from the right side of the scattering region as

$$\Phi_n^-(x,y)=\begin{cases}\xi_{n-}+\sum_{n'=1}^{N}\xi_{n'+}r'_{n'n}, & x>L\\ \sum_{n'=1}^{N}\xi_{n'-}t'_{n'n}, & x<0,\end{cases} \tag{2.7}$$

with transmission and reflection amplitudes, t'_{mn} and r'_{mn}. The scattering matrix, or the S matrix, is defined as

$$S=\begin{bmatrix}r & t'\\ t & r'\end{bmatrix}\ . \tag{2.8}$$

The current conservation law requires the unitarity of the S matrix as

$$\tilde{S}^{\dagger}\tilde{S}=\tilde{S}\tilde{S}^{\dagger}=1\ , \tag{2.9}$$

where $\tilde{S}$ consists of the $N_c\times N_c$ transmission matrices $\tilde{t}$ and $\tilde{t}'$ and the reflection matrices $\tilde{r}$ and $\tilde{r}'$, which contain the scattering amplitudes from N_c incoming conducting channels to N_c outgoing conducting channels.

To calculate the conductance between two reservoirs, we use the two-terminal, multichannel version[32–36] of Landauer's formula[37]

$$G=\frac{2e^2}{h}\mathrm{Tr}(\tilde{t}\tilde{t}^{\dagger})=\frac{2e^2}{h}\sum_{n=1}^{N_c}\sum_{m=1}^{N_c}|\tilde{t}_{mn}|^2\ , \tag{2.10}$$

where a factor 2 due to the spin degeneracy is included. Here it should be noted shortly that conductance fluctuations, though universal in the two-terminal metallic wire, are shown both theoretically[38–41] and experimentally[42,43] to exceed the universal value by many orders of magnitude in the multiterminal system.

The overall S matrix for the disordered region $L\times W$ containing a certain number of impurities with δ potential can be obtained by decomposing it into single-impurity parts and free-propagating parts using a composition law.[44] If we consider the two S matrices defined by

$$S_1=\begin{bmatrix}r_1 & t'_1\\ t_1 & r'_1\end{bmatrix}\quad\text{and}\quad S_2=\begin{bmatrix}r_2 & t'_2\\ t_2 & r'_2\end{bmatrix}\ , \tag{2.11}$$

then the composed S matrix $S_{12}\equiv S_1\otimes S_2$ for S_1 and S_2 in series can be calculated as

$$\begin{aligned}t_{12}&=t_2(1-r'_1r_2)^{-1}t_1\ ,\\ t'_{12}&=t'_1(1-r_2r'_1)^{-1}t'_2\ ,\\ r_{12}&=r_1+t'_1r_2(1-r'_1r_2)^{-1}t_1\ ,\\ r'_{12}&=r'_2+t_2r'_1(1-r_2r'_1)^{-1}t'_2\ .\end{aligned} \tag{2.12}$$

Note that the composition law satisfies the associative law $(S_1\otimes S_2)\otimes S_3=S_1\otimes(S_2\otimes S_3)$, but does not satisfy the commutative law in general, i.e., $S_2\otimes S_1\neq S_1\otimes S_2$. The overall S matrix can be expressed as

$$S=S_1^{\mathrm{free}}\otimes S_1^{\mathrm{imp}}\otimes S_2^{\mathrm{free}}\otimes\cdots\otimes S_{N_I}^{\mathrm{imp}}\otimes S_{N_I+1}^{\mathrm{free}}\ , \tag{2.13}$$

where N_I is the total number of impurities. It must be noted that this decomposition method of the disordered region into parts by Eq. (2.13) cannot be applied to the system containing impurities with the long-range potential.

Now, we derive the S matrix for a single impurity. We first integrate the Schrödinger equation for the system containing an impurity with a δ-function potential of strength γ at $\mathbf{r}_0=(x_0,y_0)$ over the infinitesimally small region $[x_0-\epsilon,x_0+\epsilon]$ with respect to x and get

$$\frac{\partial}{\partial x}\Phi(x_0+\epsilon,y)-\frac{\partial}{\partial x}\Phi(x_0-\epsilon,y)=\frac{2m\gamma}{\hbar^2}\delta(y-y_0)\Phi(x_0,y)\ . \tag{2.14}$$

Further the continuity of the wave function at $x=x_0$ leads to

$$\Phi(x_0+\epsilon,y)=\Phi(x_0-\epsilon,y)\ . \tag{2.15}$$

The wave function $\phi_{n\pm}(y)$ is expanded by an orthonormal

set of the N eigenstates ψ_j's of the reduced Hamiltonian for $B=0$.

$$\phi_{n\pm}(y)=\sum_{j=1}^{N}\psi_j(y)c_{jn}^{\pm} \tag{2.16}$$

with

$$\psi_j(y)=\begin{cases}\left[\frac{2}{W}\right]^{1/2}\sin\left[\frac{\pi j}{W}\left[y+\frac{W}{2}\right]\right], & y\le|W/2|\\ 0, & y>|W/2|.\end{cases} \tag{2.17}$$

Substituting Eqs. (2.6) and (2.16) into Eqs. (2.14) and (2.15), multiplying $\psi_{j'}^{*}(y)$, and integrating with respect to y, we have the transmission and reflection matrix, t and r, for incoming waves from the left-hand side

$$\begin{bmatrix}C_-K+i\Gamma C_- & C_+K+i\Gamma C_+\\ -C_- & C_+\end{bmatrix}\begin{bmatrix}r\\ t\end{bmatrix}=\begin{bmatrix}C_+K-i\Gamma C_+\\ C_+\end{bmatrix}, \tag{2.18}$$

with

$$\begin{aligned}(C_\pm)_{jn}&=c_{jn}^{\pm}\left[\frac{\pi\hbar}{mWv_n}\right]^{1/2},\\ (K)_{nn'}&=\frac{k_nW}{\pi}\delta_{nn'},\\ (\Gamma)_{jj'}&=\frac{m\gamma W}{\pi\hbar^2}\psi_j(y_0)^{*}\psi_{j'}(y_0).\end{aligned} \tag{2.19}$$

In the same way we can obtain the transmission and reflection matrix, t' and r', for incoming waves from the right-hand side as

$$\begin{bmatrix}C_-K+i\Gamma C_- & C_+K+i\Gamma C_+\\ -C_- & C_+\end{bmatrix}\begin{bmatrix}t'\\ r'\end{bmatrix}=\begin{bmatrix}C_-K-i\Gamma C_-\\ -C_-\end{bmatrix}. \tag{2.20}$$

Combining Eqs. (2.18) and (2.20), we finally obtain

$$S^{\mathrm{imp}}=\begin{bmatrix}C_-K+i\Gamma C_- & C_+K+i\Gamma C_+\\ -C_- & C_+\end{bmatrix}^{-1}\times\begin{bmatrix}C_+K-i\Gamma C_+ & C_-K-i\Gamma C_-\\ C_+ & -C_-\end{bmatrix}. \tag{2.21}$$

The S matrix for the free propagation from $x=x_0$ to $x=x_0+\Delta x$ is given by

$$S^{\mathrm{free}}=\begin{bmatrix}0 & \theta\\ \theta & 0\end{bmatrix},\quad(\theta)_{nn'}=e^{ik_n\Delta x}\delta_{nn'}. \tag{2.22}$$

The wave numbers $\pm k_n$ or $\pm i\kappa_n$ and the corresponding wave functions $\mathbf{c}_n^{\pm}$ are calculated as follows:[45] Substituting Eq. (2.16) into Eq. (2.3), we obtain

$$\sum_{j'=1}^{N}\left[E_j\delta_{jj'}+\frac{m}{2}\omega_c^2\langle(y-l_B^2k)^2\rangle_{jj'}\right]c_{j'}=E_Fc_j, \tag{2.23}$$

with $E_j=(\hbar^2/2m)(\pi j/W)^2$, where

$$\langle Y\rangle_{jj'}=\int dy\,\psi_j^{*}(y)Y\psi_{j'}(y). \tag{2.24}$$

Defining $d_j=(kW/\pi)c_j$, Eq. (2.23) can be rewritten as

$$\begin{bmatrix}0 & 1\\ A & B\end{bmatrix}\begin{bmatrix}c\\ d\end{bmatrix}=\frac{kW}{\pi}\begin{bmatrix}c\\ d\end{bmatrix}, \tag{2.25}$$

with

$$\begin{aligned}(A)_{jj'}&=\left[\left[\frac{k_FW}{\pi}\right]^2-j^2\right]\delta_{jj'}-\left[\frac{\hbar\omega_c}{2E_1}\right]^2\left\langle\left[\frac{\pi y}{W}\right]^2\right\rangle_{jj'},\\ (B)_{jj'}&=\frac{\hbar\omega_c}{E_1}\left\langle\frac{\pi y}{W}\right\rangle_{jj'},\end{aligned} \tag{2.26}$$

where $k_F=(2mE_F/\hbar^2)^{1/2}$. Solving Eq. (2.25), we obtain $2N$ eigenvalues $\pm k_n$ or $\pm i\kappa_n$ and $2N$ eigenvectors $\mathbf{c}_n^{\pm}$.

The situation becomes particularly simple in the absence of a magnetic field. We have $k_n=[k_F^2-(\pi n/W)^2]^{1/2}$ and $v_n=\hbar k_n/m$ when $E_n<E_F$ and $\kappa_n=[(\pi n/W)^2-k_F^2]^{1/2}$ when $E_n>E_F$. Further, we have $c_{jn}^{\pm}=\delta_{jn}$ and the S matrix (2.21) reduces exactly to the same expression as that previously obtained without evanescent states[23,24] and with evanescent states.[25,26,46]

The system is characterized by the following three dimensionless parameters: W/λ_F, $l/\lambda_F=E_F\tau/\pi\hbar$, and $\tilde{\gamma}\equiv 2m\gamma/\pi\hbar^2$, where τ is the relaxation time in 2D systems given by $\tau^{-1}=n_i|\gamma|^2m/\hbar^3$ with n_i the impurity concentration and is related to the mean free path through $l=v_F\tau$. The parameter $2W/\lambda_F$ represents the number of occupied subbands at the Fermi energy. The parameter $\tilde{\gamma}$ represents the importance of the higher-order Born scatterings from a single impurity relative to the first-order Born effect. In the limit of negligibly small γ and large concentration n_i of impurities with a fixed l (the high concentration or white-noise limit), $\tilde{\gamma}$ becomes irrelevant and the system is characterized only by the two parameters W/λ_F and l/λ_F. In the following, except for a single-impurity system, we choose $|\tilde{\gamma}|=0.2$, for which the system is nearly in the high concentration limit. In addition, equal amounts of attractive and repulsive scatterers are distributed in a sample in order to cancel out effects of energy shifts to the lowest order. The number of samples with different impurity configuration is between 2000 and 3000.

The δ-function potential can cause some problems. A typical example is a divergence associated with its bound state in the attractive case in two or three dimensional systems. The same happens in the present quantum wire and the binding energy diverges logarithmically if the number N of the basis $\psi_j(y)$ becomes infinite. Any realistic scatterers have a potential with nonzero range. Therefore, we shall introduce a cutoff E_c in such a way that N is determined by the condition $E_N<E_c$. This roughly corresponds to a cutoff of the potential range at about k_c^{-1} with $\hbar^2k_c^2/2m\sim E_c$. We shall choose $E_c\simeq 4E_F$ in the numerical examples shown in the following section.

III. NUMERICAL RESULTS

A. Single impurity

The conductance for a single impurity in the absence of a magnetic field has already been calculated by Bagwell.[46] It has been shown that for an attractive potential a quasibound state is formed below each subband bottom where the transmission probability is reduced considerably. For a repulsive scatterer no such quasibound state appears as is expected. The situation changes drastically in the presence of a magnetic field.[47,48] The bound-state energy of a single impurity can be obtained as

$$1=\frac{\gamma}{2\pi l_B^2}\sum_{\nu=0}^{\nu_{\max}}\frac{1}{E-(\nu+1/2)\hbar\omega_c}\ , \tag{3.1}$$

where $\nu_{\max}$ is a cutoff. This shows that there exist bound states (with an energy larger than each Landau-level energy) even for a repulsive impurity in 2D systems in strong magnetic fields.

An example of the calculated conductance for a single impurity with $\tilde{\gamma}=\pm 0.7$ located at the center of the wire ($y_0=0$) in a strong magnetic field ($\hbar\omega_c/E_1=10$ or $W/l_B\simeq 7$) is shown in Fig. 1. Dips can be seen both for repulsive and attractive potential. They are due to the suppression of the transmission probability of the highest conducting channels: For example, when two subbands are occupied, we have $|t_{11}|\simeq 1$ and $|t_{12}|\simeq|t_{21}|\simeq|t_{22}|\simeq 0$.

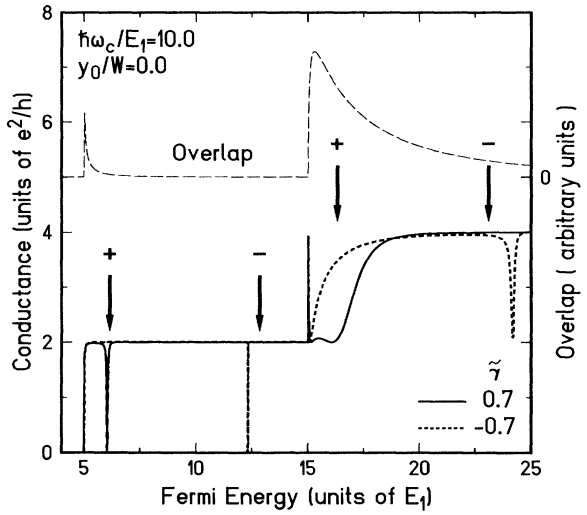

FIG. 1. Conductance for a single impurity with δ-function potential located at the center of wire ($y_0=0$) as a function of the Fermi energy in a strong magnetic field. The solid line represents that for a repulsive potential and the dotted line for an attractive potential. The conductance decreases at the energy of the quasibound states. The vertical arrows indicate the expected quasibound state energies for a 2D system with "+" for a repulsive potential and "−" for an attractive potential. The overlap between the highest conducting channels at the impurity position, $|\phi^*_{N_c-}(y_0)\phi_{N_c+}(y_0)|$, is represented by the dashed line.

The energies of quasibound states are close to those obtained from Eq. (3.1) for $\nu_{\max}=10$ shown in Fig. 1 by the vertical arrows.

The overlap of the wave functions of the highest conducting channels at the position of the impurity, $|\phi^*_{N_c-}(y_0)\phi_{N_c+}(y_0)|$, is also included in the figure. At energies away from those of quasibound states, the conductance is nearly quantized except when this overlap is large. A singular peak seen just at the energy of the bottom of the second subband ($E_F\simeq 15E_1$) is due to the presence of a node of the wave function at $y_0=0$. When E_F becomes slightly larger than the subband bottom, the overlap rapidly increases and the conductance is reduced.

B. Conductance fluctuations

In Fig. 2 we show the length dependence of the averaged conductance in the absence of a magnetic field. The narrowest wire has five occupied subbands and the widest 20 below the Fermi energy. We have assumed $l/\lambda_F=51.25$, for which the broadening is always smaller than the smallest subband separation $[\hbar/\tau=(4/\pi)(W/\lambda_F)^2(\lambda_F/l)E_1\simeq 0.87(E_2-E_1)$ even for $W/\lambda_F=10.25]$ and therefore the subbands are well resolved. The Fermi level lies in the middle of the two subband bottoms E_{N_c} and E_{N_c+1}. We have used the two different ways of averaging, the arithmetic average $\langle G\rangle$ and the geometric average $\exp[\langle \ln G\rangle]$. With the increase of the sample length, the conductance decreases starting from the quantized value $G=2N_ce^2/h$. As the system becomes much longer, the conductance begins to

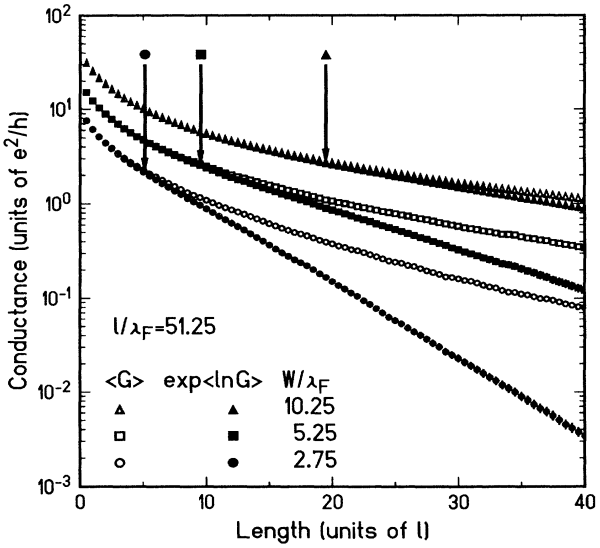

FIG. 2. Conductance as a function of the length L for different wire widths. The number of occupied subbands is $2W/\lambda_F$. When L becomes large, $\langle \ln G\rangle$ shows a linear dependence on L, from which the localization length ξ can be estimated. The estimated localization lengths are indicated by the vertical arrows. The numerical uncertainty of ξ is smaller than the width of the arrows.

decrease exponentially. The localization length ξ can be estimated by fitting to $\xi=-(\partial\langle \ln G\rangle/\partial L)^{-1}$ for the region $25<L/l<40$.[49–53] We have $\xi/l=4.9\pm0.2$ for $N_c=5$, 10.0 ± 0.3 for $N_c=10$, and 19.6 ± 1.0 for $N_c=20$, which are denoted in the figure by the vertical arrows. The two different averages start to deviate from each other when the length exceeds the localization length reflecting the well-known singular distribution of the conductance in the localized region $L\gtrsim\xi$.[49–53]

The calculation shows that ξ increases in proportion to N_c ($\xi\simeq N_c l$ within the numerical accuracy). There have been various arguments which lead to the conclusion that ξ increases in proportion to N_c in quasi-one-dimensional metallic wires. Thouless[54] has assumed that the localization length roughly corresponds to the system length L where the conductance $ne^2\tau/mL$ becomes of the order of $e^2/\pi\hbar$. The same result has been derived analytically with the use of the supersymmetry method,[55] within a model of weakly coupled 1D chains,[56] and within a random-matrix model[57] proposed by Imry[17] to explain the universal conductance fluctuations and numerically explored later.[58] Numerical calculations have also confirmed this conclusion.[59] It should be noted that in quantum wires with well-resolved 1D subbands the actual value of ξ varies considerably as a function of the energy even for a given channel number.[60]

Figure 3 shows the corresponding results for the conductance fluctuation $\delta G\equiv\langle(G-\langle G\rangle)^2\rangle^{1/2}$. With increasing length, the fluctuation first increases, takes a maximum value, and then begins to decrease. The first increase in the nearly ballistic regime is a reflection of the fact that the conductance is quantized when $L\lesssim l$, and the decreases for $L\gtrsim\xi$ is a result of the reduction of the conductance due to the localization effect. When the channel number is not so large ($W/\lambda_F=2.75$), the nearly ballistic regime and the localized regime overlap with each other and the fluctuation is always strongly dependent on the length. As the channel number increases and the localization length becomes larger, the maximum fluctuation increases and there appears a length region where the fluctuation stays independent of length (the universal region). The maximum fluctuation for $W/\lambda_F=10.25$ is close to but slightly smaller than $0.73e^2/h$ derived by the perturbational method for the quasi-one-dimensional metallic wires.[13,15]

The appearance of the universal region is not surprising because the perturbational calculation shows that the fluctuation is independent of length even in pure 1D, where, however, the localization effect is essential and the perturbation fails. With the increase of the number of occupied 1D subbands, the localization effect is reduced and there appears a finite length region where the perturbational treatment is valid and δG can be independent of length. On the other hand, it is an open question whether the absolute value of δG in the present multisubband system should be the same as that calculated perturbationally in pure 1D systems. Iwabuchi and Nagaoka have studied effects of intersubband scatterings in a 2D system with two occupied subbands and have demonstrated that the absolute value of δG is the same as that of pure 2D systems.[61]

A crossover occurs from 1D to 2D when the broaden-

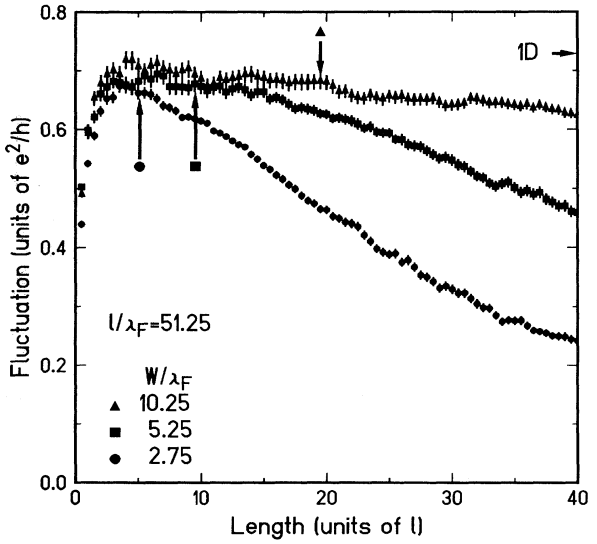

FIG. 3. Conductance fluctuations as a function of the length L for systems corresponding to those shown in Fig. 2. The universal value obtained by the perturbation for quasi-one-dimensional wires is indicated by a horizontal arrow. The localization lengths are indicated by the vertical arrows.

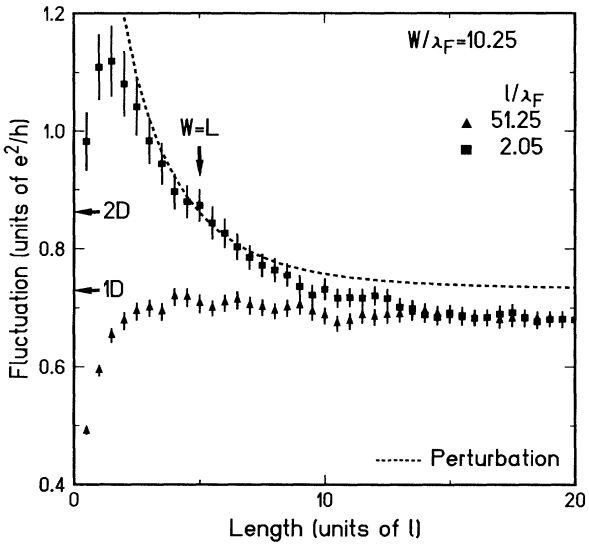

FIG. 4. A crossover of conductance fluctuations from 1D to 2D when the number of the occupied subbands is 20. The solid squares correspond to a wire where the broadening is larger than the level separation and the subband structure is smeared out. They are close in the region $3l\lesssim L\lesssim 10l$ to the dotted line obtained by the perturbation calculation for metallic wires. The triangles are the same data as those in Fig. 2. The vertical arrow indicates the length corresponding to the 2D square. The universal values obtained by the perturbation for quasi-one-dimensional wires and 2D squares are indicated by the horizontal arrows.

ing of the subbands exceeds their separation and the subband structure is smeared out. Figure 4 shows calculated δG for $l/\lambda_F=2.05$ together with that for $l/\lambda_F=51.25$ in the case that the number of occupied subbands is 20. For $l/\lambda_F=2.05$ the situation is closer to that of metallic wires, i.e., the broadening is larger than the largest subband separation $[\hbar/\tau \simeq 1.6(E_{N_c+1}-E_{N_c})]$ and the wire width is larger than the mean free path ($W/l=5$). The numerical result is in good agreement with that by the perturbation represented by the dotted line in the region $2l<L<10l$ including the length corresponding to the 2D square $W=L$. When the length is larger than $\sim 10l$, the fluctuation becomes smaller due to the localization effect.

A brief comment on effects of the evanescent states is worthwhile. The evanescent states correspond to virtual processes in scatterings. Therefore, by their inclusion the higher-order Born scatterings from a single impurity can automatically be taken into account. The major part of the effects noted in recent papers[25,26] is probably those of such higher-order Born scatterings. In this paper, we have chosen $\bar{\gamma}$ as small as possible (and also assumed equal amounts of attractive and repulsive impurities) in order to reduce the higher-order Born effects. Consequently, the evanescent states have little influence on the conductance except when the Fermi level lies just below the bottom of an excited subband, where the subband broadening cannot otherwise be treated properly. In fact, the calculated conductance suffers little change even if the evanescent states are completely neglected, when the Fermi level lies in the middle of the bottoms of two adjacent subbands.

C. Magnetic field

An example of calculated conductance as a function of the magnetic field is shown in Fig. 5. We consider a system characterized by $W/\lambda_F=2.75$ and $l/\lambda_F=51.25$ with fixed length $L=3l$, where the fluctuation becomes nearly maximum in the absence of magnetic fields, and we vary the magnetic field at a fixed value of the Fermi energy. In the presence of very weak magnetic fields ($\hbar\omega_c/E_F \lesssim 1\times 10^{-2}$), the conductance increases slightly from the value at zero field probably due to a reduction in the weak localization effect. At higher magnetic fields, the conductance exhibits an oscillatory dependence on the field.

This behavior can be understood simply in terms of the magnetic-field dependence of the mean free path. The mean free path of each subband[62] is shown in Fig. 6. Whenever the Fermi level is close to a subband bottom, the mean free path decreases drastically due to the divergence in the 1D density of states. The decrease in the conductance at each subband bottom corresponds to this strong enhancement of scattering effects. Except at such magnetic fields the mean free path increases gradually with magnetic field. In magnetic fields, electrons are pushed toward the wire edges, the overlap between wave functions associated with positive and negative velocity becomes small, and backscattering rates are lowered. At the magnetic field ($\hbar\omega_c/E_F \approx 0.4$) where the channel number changes from 3 to 2, the mean free path increases by several orders of magnitude and exceeds the system length. Correspondingly, the conductance rapidly approaches the quantized value $G=2N_c e^2/h$. In such a strong field well-defined edge states are formed and the backscatterings between the edge states are completely suppressed. An electron in the edge states can move ballistically through the sample except when the energy is in the region of broadened bulk Landau levels where the edge states are strongly mixed with the bulk levels.[60] Edge states with a long mean free path in high magnetic fields have been the recent subject of both theoretical[34,63]

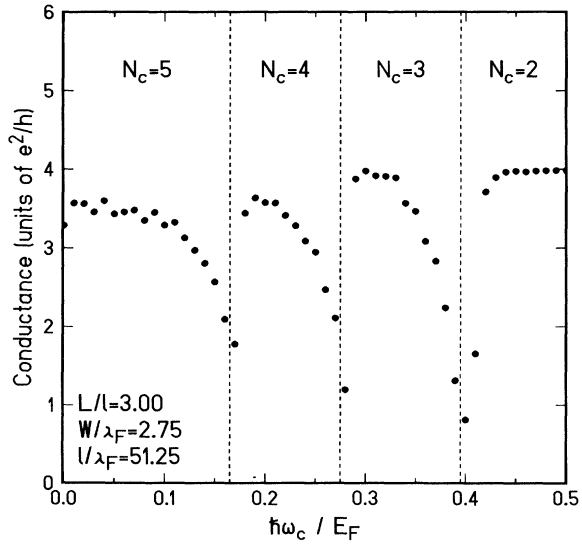

FIG. 5. Conductance as a function of the magnetic field for $L/l=3$ and $W/\lambda_F=2.75$. The number of occupied subbands N_c changes at the magnetic fields indicated by the vertical dotted lines.

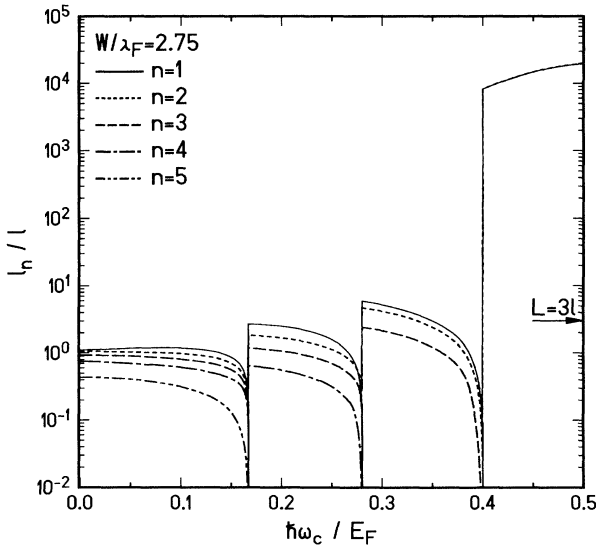

FIG. 6. Mean free path of each subband as a function of the magnetic field for the same system as that in Fig. 5.

and experimental[64–66] investigations.

Figure 7 shows the corresponding result of the fluctuation. The reduction in the fluctuation which can be seen in weak magnetic fields ($\hbar\omega_c/E_F \lesssim 1\times10^{-2}$) corresponds to the suppression of the contribution from the so-called "particle-particle channel" predicted by perturbational calculations.[12–15] As a matter of fact, the flux penetrating through the sample is $BLW \sim 13h/e$ for $\hbar\omega_c/E_F \sim 1\times10^{-2}$. When the magnetic field is increased further, the fluctuation gradually decreases except in the vicinity of the fields where the subband depopulation occurs. This can be explained by the gradual approach of the system to the ballistic regime due to the increase in the mean free path. In strong magnetic fields ($\hbar\omega_c/E_F \gtrsim 0.45$) the fluctuation becomes negligibly small corresponding to the quantization of the conductance itself.

Figure 8 shows G as a function of L for $W/\lambda_F=5.25$ and $l/\lambda_F=51.25$ in the weak field $\hbar\omega_c/E_F=3\times10^{-3}$ together with G at $B=0$. In terms of the magnetic flux, each area normal to the field with length l and width W is penetrated by $BlW/(h/e)=2.5$ flux. In the magnetic field the conductance becomes larger than that at $B=0$ at every length due to the reduction of the localization effect. The localization length, denoted by the vertical arrow, is 16.7 ± 0.6 in units of l smaller than twice of the value at $B=0$. This decrease of the localization effect is a result of the change in the universality class of the system from orthogonal to unitary, i.e., due to the breaking of the time-reversal symmetry by a magnetic field. This fact has been shown in various methods.[67–69] The exact doubling of the localization length in quasi-one-dimensional metallic wires in magnetic fields has been suggested by various methods.[55–57]

Figure 9 shows the corresponding results for the fluctuation. The universal region can now be clearly seen as

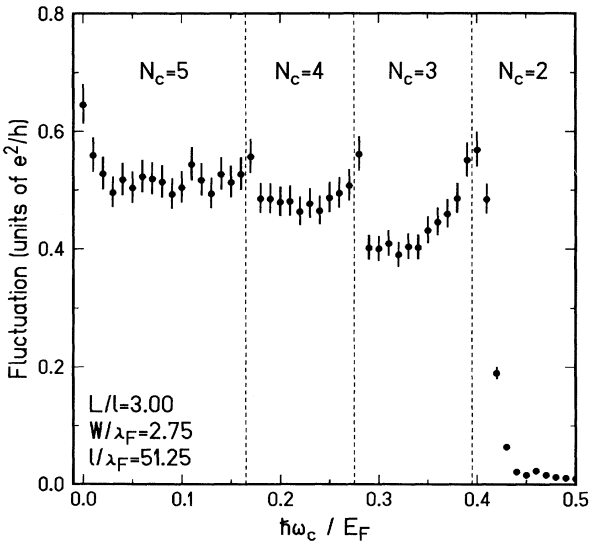

FIG. 7. The fluctuations as a function of the magnetic field for the same system as that in Fig. 5.

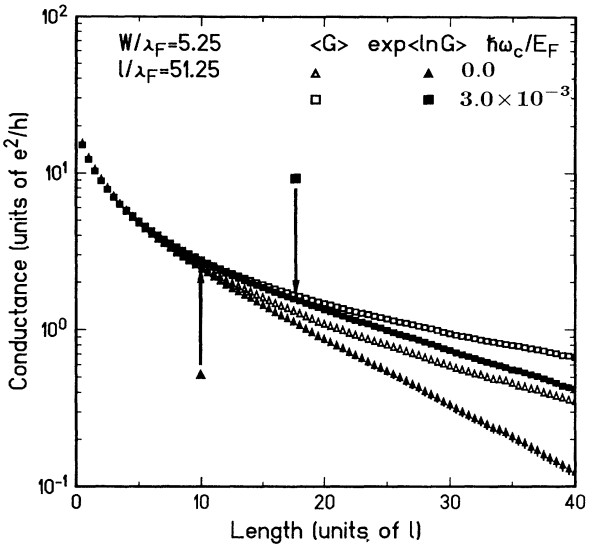

FIG. 8. Conductance as a function of the length L for $W/\lambda_F=5.25$ in the magnetic field corresponding to $\hbar\omega_c/E_F=3\times10^{-3}$ compared with that at $B=0$. The magnetic flux penetrating through the area with length l and width W is $BlW=2.5h/e$. The localization lengths are indicated by the vertical arrows.

well as the reduction of δG in comparison with δG at $B=0$, when the sample is shorter than the localization length ($L<15l$). The actual amount of the reduction is slightly smaller than that predicted by perturbational calculations $[\delta G(B)/\delta G(B=0)\simeq0.8$ in contrast to

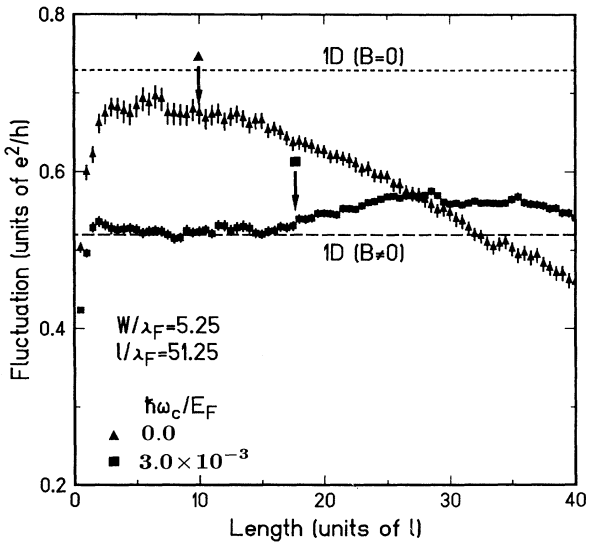

FIG. 9. Conductance fluctuations as a function of L in the presence of the magnetic field compared with those at $B=0$ for the same system as that in Fig. 8. The localization lengths are indicated by the vertical arrows. The universal values obtained by the perturbation calculation in quasi-one-dimensional wires are indicated by the horizontal dotted line ($B=0$) and the dashed line ($BLW \gg h/e$).

$1/\sqrt{2}=0.71$]. This difference is to be expected because the mechanism leading to the reduction is absent in pure 1D wires with a single occupied subband. When the sample becomes longer than the localization length, δG somewhat increases and then begins to decrease in the region $L > 35l$. It is quite interesting that the magnetic field enhances δG in the localized regime, while it reduces δG in the universal region.

IV. SUMMARY AND CONCLUSION

In conclusion, we have calculated conductance fluctuations in quantum wires both in the absence and in the presence of magnetic fields. It has been shown that with increasing length L the fluctuations increase in the region $L \lesssim l$ with l the mean free path and start to decrease when L exceeds the localization length ξ. When only a few subbands are occupied, ξ is comparable to l and there is no universal region where the fluctuations stay independent of L. When many subbands are occupied, ξ is much larger than l ($\xi \simeq N_c l$ with N_c the number of occupied subbands) and there appears a universal region for $l \lesssim L \lesssim \xi$. The absolute value of the fluctuation in the universal region is close to that obtained for quasi-1D systems by the perturbational method. We have also demonstrated that the dimensional crossover from 1D to 2D systems or from quantum wires to metallic wires occurs when the broadening exceeds the subband energy separations. In the presence of a weak magnetic field, the universal region becomes wider due to the reduction in the localization effect and the fluctuation itself is reduced. In strong magnetic fields where edge states with an extremely long mean free path are formed, the conductance is almost quantized and the fluctuation nearly vanishes.

ACKNOWLEDGMENTS

We would like to thank H. Akera for useful discussions. This work is supported in part by the Industry-University Joint Research Program "Mesoscopic Electronics" and by a Grant-in-Aid for Scientific Research on Priority Area "Electron Wave Interference Effects in Mesoscopic Structures" from the Ministry of Education, Science and Culture, Japan.

[1]For a review, see S. Washburn and R. A. Webb, Adv. Phys. **35**, 375 (1986), and references therein.
[2]C. P. Umbach, S. Washburn, R. B. Laibowitz, and R. A. Webb, Phys. Rev. B **30**, 4048 (1984).
[3]Y. Gefen, Y. Imry, and M. Ya. Azbel, Phys. Rev. Lett. **52**, 129 (1984).
[4]M. Büttiker, Y. Imry, and M. Ya. Azbel, Phys. Rev. A **30**, 1982 (1984).
[5]M. Büttiker, Y. Imry, R. Landauer, and S. Pinhas, Phys. Rev. B **31**, 6207 (1985).
[6]R. A. Webb, S. Washburn, C. P. Umbach, and R. B. Laibowitz, Phys. Rev. Lett. **54**, 2696 (1985).
[7]G. Timp, A. M. Chang, P. Mankiewich, R. Behringer, J. E. Cunningham, T. Y. Chang, and R. E. Howard, Phys. Rev. Lett. **59**, 732 (1987); A. M. Chang, G. Timp, T. Y. Chang, J. E. Cunningham, P. M. Mankiewich, R. E. Behringer, and R. E. Howard, Solid State Commun. **67**, 769 (1988).
[8]M. L. Roukes, A. Scherer, S. J. Allan, Jr., H. G. Craighead, R. M. Ruthen, E. D. Beebe, and J. P. Harbison, Phys. Rev. Lett. **59**, 3011 (1987).
[9]C. J. B. Ford, T. J. Thornton, R. Newbury, M. Pepper, H. Ahmed, D. C. Peacock, D. A. Ritchie, J. E. F. Frost, and G. A. C. Jones, Phys. Rev. B **38**, 8518 (1988).
[10]B. J. van Wees, H. van Houten, C. W. J. Beenekkar, J. G. Williamson, L. P. Kouwenhoven, D. van der Marel, and C. T. Foxon, Phys. Rev. Lett. **60**, 848 (1988).
[11]D. A. Wharam, T. J. Thornton, R. Rewbury, M. Pepper, H. Ahmed, J. E. F. Frost, D. G. Hasko, D. C. Peacock, D. A. Ritchie, and G. A. C. Jones, J. Phys. C **21**, L209 (1988).
[12]B. L. Altshuler, Pis'ma Zh. Eksp. Theor. Fiz. **41**, 530 (1985) [JETP Lett. **41**, 648 (1985)].
[13]P. A. Lee and A D. Stone, Phys. Rev. Lett. **55**, 1622 (1985).
[14]B. L. Altshuler and D. E. Khmelnitshii, Pis'ma Zh. Eksp. Theor. Fiz. **42**, 291 (1985) [JETP Lett. **42**, 359 (1986)].
[15]P. A. Lee, A. D. Stone, and H. Fukuyama, Phys. Rev. B **35**, 1039 (1987).
[16]C. L. Kane, R. A. Serota, and P. A. Lee, Phys. Rev. B **37**, 6701 (1988).
[17]Y. Imry, Europhys. Lett. **1**, 249 (1986).
[18]A. D. Stone, Phys. Rev. Lett. **54**, 2692 (1985).
[19]N. Giordano, Phys. Rev. B **36**, 4190 (1987).
[20]X. C. Xie and S. Das Sarma, Phys. Rev. B **38**, 3529 (1988).
[21]K. Tankei, A. Sawada, and Y. Nagaoka, J. Phys. Soc. Jpn. **58**, 368 (1989).
[22]B. Kramer, J. Masek, V. Spicka, and B. Velicky, Surf. Sci. **229**, 316 (1990).
[23]S. Datta, M. Cahay, and M. McLennan, Phys. Rev. B **36**, 5655 (1987).
[24]M. Cahay, M. McLennan, and S. Datta, Phys. Rev. B **37**, 10 125 (1988).
[25]M. Cahay, S. Bandyopadhyay, M. A. Osman, and H. L. Grubin, Surf. Sci. **228**, 301 (1990).
[26]S. Bandyopadhyay, M. Cahay, D. Berman, and B. Nayfeh, in Proceedings of the Fifth International Conference on Superlattices and Microstructures, Berlin, 1990 [Supperlatt. Microstruct. (to be published)].
[27]R. Harris and A. Houari, Phys. Rev. B **41**, 5487 (1990).
[28]D. J. Thouless, J. Phys. C **6**, L49 (1973).
[29]K. Ishii, Prog. Theor. Phys. **53**, 77 (1973).
[30]P. Erdös and R. C. Herndon, Adv. Phys. **31**, 65 (1982).
[31]H. Sakaki, Jpn. J. Appl. Phys. **19**, L735 (1980).
[32]D. S. Fisher and P. A. Lee, Phys. Rev. B **23**, 6851 (1981).
[33]M. Büttiker, Phys. Rev. Lett. **57**, 1761 (1986).
[34]M. Büttiker, Phys. Rev. B **38**, 9375 (1988).
[35]A. D. Stone and A. Szafer, IBM J. Res. Develop. **32**, 384 (1988).
[36]H. U. Baranger and A. D. Stone, Phys. Rev. B **40**, 8169 (1989).
[37]R. Landauer, IBM J. Res. Develop. **1**, 223 (1957); Philos. Mag. **21**, 863 (1970).
[38]Y. Isawa, H. Ebisawa, and S. Maekawa, J. Phys. Soc. Jpn. **55**, 2523 (1986); S. Maekawa, Y. Isawa, and H. Ebisawa, *ibid.* **56**, 25 (1987); Y. Isawa, H. Ebisawa, and S. Maekawa, in *Ander-*

son Localization, edited by T. Ando and H. Fukuyama (Springer-Verlag, Berlin, 1988), p. 329.
[39]M. Büttiker, Phys. Rev. B **35**, 4123 (1987).
[40]H. U. Baranger, A. D. Stone, and D. P. DiVincenzo, Phys. Rev. B **37**, 6521 (1988), C. L. Kane, P. A. Lee, and D. P. DiVincenzo, *ibid.* **38**, 2995 (1988), D. P. DiVincenzo and C. L. Kane, *ibid.* **38**, 3006 (1988).
[41]S. Hershfield and V. Ambegaokar, Phys. Rev. B **38**, 7909 (1988). S. Hershfield, Ann. of Phys. **196**, 12 (1989).
[42]A. Benoit, C. P. Umbach, R. B. Laibowitz, and R. A. Webb, Phys. Rev. Lett. **58**, 2343 (1987).
[43]W. J. Skocpol, P. M. Mankiewich, R. E. Howard, L. D. Jackel, D. M. Tennant, and A. D. Stone, Phys. Rev. Lett. **58**, 2347 (1987).
[44]P. W. Anderson, Phys. Rev. B **23**, 4828 (1981).
[45]See, for example, Y.-C. Chang, and J. N. Schulman, Phys. Rev. B **25**, 3975 (1982); **31**, 2069 (1985), and references cited therein.
[46]P. F. Bagwell, Phys. Rev. B **41**, 10 354 (1990).
[47]T. Ando and Y. Uemura, J. Phys. Soc. Jpn. **36**, 959 (1974).
[48]T. Ando, J. Phys. Soc. Jpn. **36**, 1521 (1974); **37**, 622 (1974); **37**, 1233 (1974).
[49]P. W. Anderson, D. J. Thouless, E. Abrahams, and D. S. Fisher, Phys. Rev. B **22**, 3519 (1980).
[50]E. Abrahams and M. J. Stephen, J. Phys. C **13**, L377 (1980).
[51]B. S. Andereck and E. Abrahams, J. Phys. C **13**, L383 (1980).
[52]J. Sak and B. Kramer, Phys. Rev. B **24**, 1761 (1981).
[53]A. D. Stone, J. D. Joannopoulos, and D. J. Chadi, Phys. Rev. B **24**, 5583 (1981).
[54]D. J. Thouless, Phys. Rev. Lett. **39**, 1167 (1977).
[55]K. B. Efetov and A. I. Larkin, Zh. Eksp. Theor. Fiz. **85**, 764 (1983) [Sov. Phys. JETP. **58**, 444 (1983)].
[56]O. N. Dorokhov, Zh. Eksp. Theor. Fiz. **85**, 1040 (1983) [Sov. Phys. JETP. **58**, 606 (1983)].
[57]J.-L. Pichard, M. Sanquer, K. Slevin, and P. Debray, Phys. Rev. Lett. **65**, 1812 (1990).
[58]A. D. Stone, K. A. Muttalib, and J.-L. Pichard, in *Anderson Localization,* edited by T. Ando and H. Fukuyama (Springer-Verlag, Berlin, 1988), p. 315; K. A. Muttalib, J.-L. Pichard, and A. D. Stone, Phys. Rev. Lett. **59**, 2475 (1987).
[59]A. MacKinnon and B. Kramer, Phys. Rev. Lett. **47**, 1546 (1981).
[60]T. Ando, Phys. Rev. B **42**, 5626 (1990).
[61]S. Iwabuchi and Y. Nagaoka, in *Proceedings of the Third International Symposium on Foundations of Quantum Mechanics,* edited by S. Kobayashi, H. Ezawa, Y. Murayama, and S. Nomura (Physical Society of Japan, Tokyo, 1990), p. 288.
[62]See, for example, H. Akera and T. Ando, Phys. Rev. B **41**, 11 967 (1990).
[63]T. Martin and S. Feng, Phys. Rev. Lett. **64**, 1971 (1990).
[64]S. Komiyama, H. Hirai, S. Sasa, and T. Fujii, Solid State Commun. **73**, 91 (1990).
[65]B. W. Alphenaar, P. L. McEuen, R. G. Wheeler, and R. N. Sacks, Phys. Rev. Lett. **64**, 677 (1990).
[66]B. L. van Wees, E. M. M. Willems, L. P. Kouwenhoven, C. J. P. M. Harmans, J. G. Williamson, C. T. Foxon, and J. J. Harris, Phys. Rev. B **39**, 8066 (1989).
[67]P. A. Lee and D. S. Fisher, Phys. Rev. Lett. **47**, 882 (1981).
[68]U. Krey, W. Maass, and J. Stein, Z. Phys. B **49**, 199 (1982).
[69]T. Ando, Phys. Rev. B **40**, 5326 (1989).